ENVIRONMENTAL RESEARCH
LETTERS

LETTER • OPEN ACCESS

Asymmetry variations in Arctic summer onset and ending: Role of sea-ice melting

To cite this article: Xiaoye Yang *et al* 2022 *Environ. Res. Lett.* **17** 114039

IOP Publishing Environ. Res. Lett. 17 (2022) 114039 https://doi.org/10.1088/1748-9326/ac9dad

ENVIRONMENTAL RESEARCH
LETTERS

LETTER

Asymmetry variations in Arctic summer onset and ending: Role of sea-ice melting

Xiaoye Yang[1], Gang Zeng[1,*], Wei-Chyung Wang[2], Vedaste Iyakaremye[1,3] and Shiyue Zhang[1]

[1] Key Laboratory of Meteorological Disaster of Ministry of Education (KLME), Collaborative Innovation Center on Forecast and Evaluation of Meteorological Disasters (CIC-FEMD), Nanjing University of Information Science and Technology, Nanjing, People's Republic of China
[2] Atmospheric Sciences Research Center, University at Albany, State University of New York, Albany, NY, United States of America
[3] Rwanda Meteorology Agency, Kigali, Rwanda
[*] Author to whom any correspondence should be addressed.

E-mail: zenggang@nuist.edu.cn

Keywords: Arctic, sea ice, summer onset, summer ending, asymmetry variations

Supplementary material for this article is available online

OPEN ACCESS

RECEIVED
17 July 2022

REVISED
10 October 2022

ACCEPTED FOR PUBLICATION
26 October 2022

PUBLISHED
7 November 2022

Abstract

Previous studies found that in Arctic regions with severe sea ice melting, summer ending (SE) variations are significantly larger than summer onset (SO) variations in the past few decades. Based on short-term observations, researchers preliminarily suggested that radiation variations caused by an earlier melting onset could be the possible reason for asymmetric Arctic SO/ending variations (AASV). Based on observations and National Centers for Environmental Prediction/National Center for Atmospheric Research (NCEP/NCAR) Reanalysis I dataset, here we quantitatively characterize AASV by calculating the difference between the 11 year sliding trend of Arctic SO and SE. The results show that AASV positively correlates with sea ice melting in summer. The increased summer sea ice melting increases the area to absorb short-wave radiation in summer and then release more long-wave radiation to heat the lower atmosphere and delay the peak time of long-wave radiation releasing. The variations in radiation lead to a significant delay of the Arctic SE, with no significant variations in SO. We introduce CMIP6 historical and future simulations of 15 models to verify further the relationship between AASV and summer sea ice melting. Historical run reproduces the observed asymmetry, and future simulations under various warming levels show that AASV will vanish with disappeared melting variations or be strengthened with increased melting. The latter could delay freeze-up and further exacerbate the following years' melting, which will enhance AASV. Furthermore, AASV will delay the onset and peak time of Arctic amplification.

1. Introduction

The sustained decline of sea ice has caused widespread concerns in recent years. The sea ice loss occurred in all months, with the strongest in late summer and the weakest in winter (Stroeve *et al* 2014). Since satellite records began in 1979, the Arctic sea-ice extent (SIE) in September has decreased by ∼50% (Stroeve and Notz 2018), accompanied by a significant decline in thickness (Kwok *et al* 2009), which may be linked to the prolonged Arctic summer melting season (Perovich and Polashenski 2012, Stroeve *et al* 2014).

Pinpointing the timing of the Arctic melting season is challenging (Markus *et al* 2009, Stroeve *et al* 2014, Huang *et al* 2017). Previous studies determined the onset of the melting and freezing season with satellite passive microwave data or other instrument data by calculating the daily melting (Markus *et al* 2009, Biss and Anderson 2014, Stroeve *et al* 2014, Serreze *et al* 2016). Based on these data, researchers found that variations of Arctic summer melting season onset is about twice that of the ending (Serreze and Stroeve 2015), which we summarized as the asymmetric Arctic summer onset (SO)/ending variations (AASV). The asymmetry is not invariable, but strengthened after the mid-1990s (Stroeve and Notz 2018). Notably, this asymmetry between SO variations and summer ending (SE) variations occurs only in the Arctic, especially in areas with significant summer sea ice decline, including Barents, Kara, Laptev, East Siberian, Chukchi, and Beaufort seas (Stroeve *et al* 2014).

The increase in air temperature under global warming may be an important cause of the sea ice loss and the prolonged summer (Perovich and Polashenski 2012, Notz and Stroeve 2016, Ding *et al* 2017). However, when the decline of SIE occurs, a series of feedback processes may further aggravate the sea ice loss (Screen and Simmonds *et al* 2010, Taylor *et al* 2013) and amplify AASV. (Perovich *et al* (2008), Perovich *et al* (2011)) found that the total amount of solar energy absorbed during the summer was closely related to the melting onset. The earlier melting onset leads to the earlier development of ice-free areas that, in turn, enhance the ice-albedo feedback. As a result, the sea areas with melting sea ice can further release more long-wave radiation to heat the lower atmosphere during the subsequent cool season, which may be considered as an important reason for Arctic amplification effect appearing in the cool season (Dai *et al* 2019). Studies suggested that the amount of solar energy absorbed in summer could largely explain the observed delays in SE, and attribute the variations of the former to an earlier melting onset (Markus *et al* 2009, Stroeve *et al* 2014).

Limited by a single trend of sea ice melting variations and the difficulty in capturing the variations of AASV through short-term observations, the relationship between summer melting trend and AASV is less discussed. Thus, the following key research questions are still open (a) why does the strong AASV only appear in the Arctic? (b) how is it related to the melting Arctic sea ice? and (c) what are the most probable consequences? We need to find an alternative dataset that could overcome the melting's limited short-term observations to answer these questions. Therefore, we use surface air temperature (SAT) to determine the Arctic SO and SE, and introduce coupled model intercomparison project phase 6 (CMIP6) simulations to explore the long-term relationship between AASV and Arctic sea ice melting variations and the influence of AASV. The rest of this paper is structured as follows. Section 2 introduces the data and methods. Section 3 shows the obtained results from observations and simulations, and section 4 presents the conclusions and discussion.

2. Data and methods

2.1. Data

This study uses the daily National Centers for Environmental Prediction/National Center for Atmospheric Research (NCEP-NCAR) Reanalysis-I dataset (Kalnay *et al* 1996), including the SAT, net short-wave radiation (NSWR), and clear sky upward longwave radiation (ULWR) from 1979 to 2020. We also use daily SAT data of 31 meteorological stations in the Arctic region obtained from the World Meteorological Organization (WMO) website (http://climexp.knmi.nl/showmap.cgi), monthly satellite data of NSWR and ULWR from the Clouds and the Earth's Radiant Energy System Energy Balanced and Filled, Top of Atmosphere Edition-4.1 (https://ceres.larc.nasa.gov/), and daily Arctic SIE from National Snow & Ice Data Center (https://nsidc.org/) to validate reanalysis results.

Table 1. Basic information (name and group) and atmospheric resolution (latitude × longitude, presented in grid points) of 15 CMIP6 global climate models.

No	Model name	Group	Atmospheric resolution
1	ACCESS-CM2	CSIRO/Australia	144 × 192
2	BCC-CSM2-MR	BCC/China	160 × 320
3	CanESM5	CCCma/Canada	64 × 128
4	CESM-WACCM	NCAR/USA	192 × 288
5	CMCC-CM2-SR5	CMCC/Italy	192 × 288
6	CMCC-ESM2	CMCC/Italy	192 × 288
7	EC-Earth3	EC-Earth-Consortium/Europe	256 × 512
8	IPSL-CM6A-LR	IPSL/France	143 × 144
9	MIROC6	MIROC/Japan	128 × 256
10	MPI-ESM1-2-HR	MPI-M/Germany	192 × 384
11	MPI-ESM1-2-LR	MPI-M/Germany	96 × 192
12	MRI-ESM2-0	MRI/Japan	160 × 320
13	NESM3	NUIST/China	96 × 192
14	NorESM2-LM	NCC/Norway	96 × 144
15	NorESM2-MM	NCC/Norway	192 × 288

To explore the long-term feedback between AASV and sea ice melting, we use daily SAT and monthly sea ice concentration (SIC) data from historical (1979–2014) and future (2015–2100) simulations from the CMIP6 under various Shared Socioeconomic Pathways scenario. The scenarios considered here are low (SSP1-2.6), middle (SSP2-4.5), and high (SSP5-8.5). SSP5-8.5 consists high enough emission SSP scenario (SSP5) to generate a radiative forcing of 8.5 Wm^{-2} in 2100. SSP2-4.5 combines medium societal vulnerability (SSP2) with a forcing of 4.5 Wm^{-2}. SSP1-2.6 combines low vulnerability with low challenges for mitigation (SSP1) as well as a low forcing of 2.6 Wm^{-2}. 15 models, which include the required historical and future data (daily SAT and SIC data), were selected (table 1). Other models are not selected because they cannot meet the required daily data. The SIC was remapped onto 1° × 1°, and all the other data were interpolated to a 2.5° grid using a bilinear interpolation scheme. In addition, we performed an independent analysis of the first simulation results for each model and then averaged all models with equal weighting to get the multi-model ensemble mean results.

2.2. Definition

Following previous studies (Huang *et al* 2017, Francis and Wu 2020), the Arctic SIE is defined as the area with >15% ice concentration. However, there are challenges in determining the division of the Arctic seasons (Stroeve *et al* 2014, Serreze *et al* 2016). Since the methods used in previous studies to determine the onset of arctic melting by satellite passive microwave

data are difficult to reproduce in CMIP6 simulations, we identify the Arctic summer through SAT. Referring to the seasonal division in mid-latitudes (Wang *et al* 2021), the Arctic SO and SE in this paper are defined as the day when the daily SAT exceeds (below) the 75th percentile of the 1979–2014 mean daily temperature. The rest of the year is the non-summer days. It should be noted that, in the observation results, the summer SO/SE identified by using SAT is close to that identified by using microwave data (about 10 d) in previous studies (Markus *et al* 2009, Stroeve *et al* 2014).

We calculate the 11 year sliding trend of non-summer days in the first half year and non-summer days in the second half year and then multiply the sliding trend by −1 to represent the SO and SE variations, respectively. A positive trend means the summer tends to be prolonged. The higher the trend, the earlier (later) the SO (SE). Therefore, the AASV can be quantified by calculating the difference between SE and SO variations. This approach allows us to capture the AASV variations and further investigate their relationship with sea ice melting. The summer sea ice melting is obtained by taking the difference between the SIE at SE and that at SO. The Arctic Amplification index is calculated as the 21 years sliding ratio of surface temperature trends between the Arctic and the rest of the northern hemisphere (Johannessen *et al* 2016, Davy *et al* 2018). It should be noted that the main results of this paper are not sensitive to the threshold.

3. Results

3.1. Observed results

With the significant rise of SAT, the length of the worldwide summer has prolonged in recent decades, as it is in the Arctic. However, only in the Arctic do the SO and SE reflect the asymmetry, which means the delay of the SE is much more apparent than the early arrival of the SO in the Arctic (figures 1(a) and (b)), unlike anywhere else in Northern Hemisphere (NH). The observed and reanalyzed variations of SAT (figure 1(d)) and the daily melting of satellite records (Stroeve *et al* 2014) can capture this asymmetry. This asymmetry occurred especially in areas where Arctic sea ice melted significantly after the mid-1990s, including Barents, Kara, Laptev, East Siberian, Chukchi, and Beaufort seas. Therefore, we set these sea areas as key regions (Abbreviated as KR, ranging from 20°W, 70°N east to 140°W, 80°N) to explore the relationship between AASV and sea ice melting. Figure 1(e) shows little change in the SO in KR, while the SE is significantly delayed after the mid-1990s, contributing to the AASV. The asymmetry can also be found in most meteorological observation stations in KR (figure 1(d)). In addition, we note that before the mid-1990s, the SE variations is negative in KR (figure 1(e)), especially in the Barents Sea (figure S1(b)). This feature is related to the negative phase of Atlantic Multidecadal Oscillation (AMO), which can influence the anomalous oceanic heat transport toward the Arctic (Miles *et al* 2014, Zhang 2015) and regulate the sea ice melting in the sector of the Arctic by affecting the atmospheric blocking frequency over the Euro-Atlantic sector (Peings and Magnusdottir 2014, Omrani *et al* 2016). Similar variations could be found in Arctic SIE at the SO and SE, which may be related to the total freshwater inflow affected by AMO (Sun *et al* 2015).

The AASV is significantly correlated with the summer sea ice melting from SO to SE, and the correlation coefficient is as high as 0.48 (figure 2(a)). It should be noted that the correlation coefficient between the two is 0.37 (0.44) after removing the linear trend during 1979–2020 (1996–2020). It indicates that their relationship may be affected by global warming and AMO. The shrinking SIE increases the ice-free sea areas with low albedo, enhancing the ability to absorb short-wave radiation during the summer. The energy is stored in the upper oceans and could be released through longwave radiation to heat the lower atmosphere in subsequent days (figures 2(b) and (c)). It can be found that, especially after the mid-1990s, the shortwave radiation absorbed in KR during June-July-August has increased significantly due to the increase of sea ice melting. Accordingly, more longwave radiation has been released to heat the lower-level atmosphere after September, which is an important reason for the delay of the SO. On the other hand, the lagged response time of the longwave radiation release to shortwave radiation absorption becomes longer, which can be found by the lag time variations in the maximum correlation coefficient between ULWR and NSWR (figure 2(d)). These variations in radiation well matched the spatial distribution and could be captured from reanalysis data and satellite observations (figure S2). Limited by short-term observations and monotonic trends in AASV and summer sea ice melting, it is hard to capture the variations of AASV, and here we introduce various scenario simulations from CMIP6.

3.2. Simulated results

Historical simulations of 15 models consistently reproduce the observed asymmetry. Although the intensity of asymmetry varies between the models, the averaged AASV in historical simulations also increased since the mid-1990s (figure S3). Under SSP1-2.6, SSP2-4.5, and SSP5-8.5 scenarios, summers have lengthened significantly in both the NH and KR as expected (figures 3(a)–(c)). The earlier SO and the delayed SE both contributed. It can be found that the summer variations are more obvious in the Arctic than that in the NH the warming scenario intensifies (figures 3(d)–(f)). Under the SSP1-2.6 scenario, the SO variations in the KR region is close to zero, and the

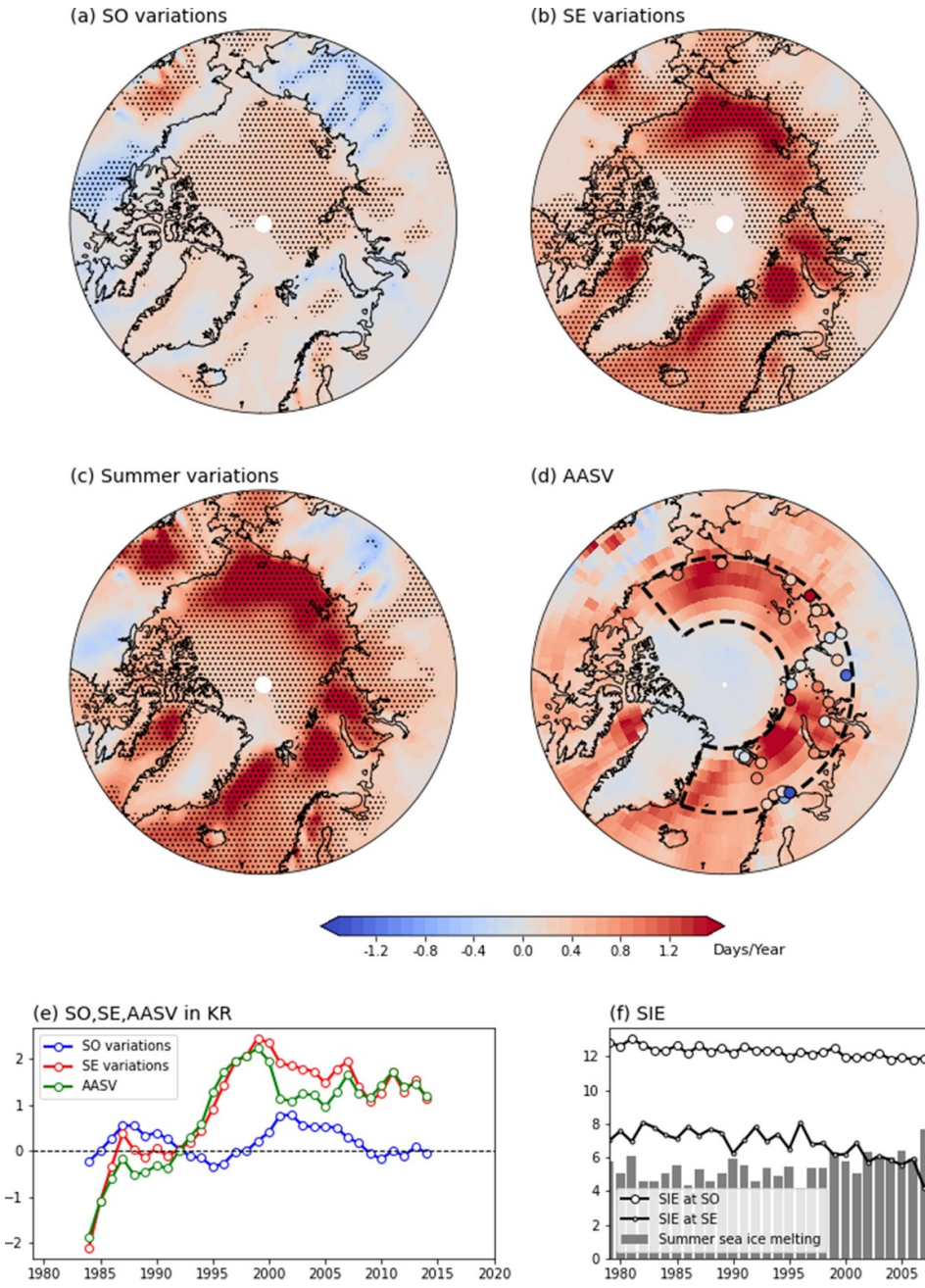

Figure 1. The mean (a) SO variations, (b) SE variations, and (c) summer length variations from 1979 to 2020 (in unit of days/year). Dotted areas show significant values at the 99% confidence level. (d) AASV, the difference between (b) and (a). The 31 shading circles denote the meteorological site observation data, and the dotted box highlights the KR. (e) Series of SO variations, SE variations and AASV in KR. (f) The SIE (in unit of 10^6 km^2) at SO and at SE, and Summer Sea ice melting in Arctic.

SE variations gradually decreased, and disappeared after the middle of the 21st century (figure 3(g)). Under the SSP2-4.5 scenario, the SO variations are slightly higher than 0 in the 21st century, and the positive SE variations decrease in the late 21st century (figure 3(h)). While under the SSP5-8.5 scenario, the SO and SE variations continued to increase (figure 3(i)).

To further investigate the correlation and causal relationship between the AASV and SIE in KR, we calculate the AASV (brown lines in figures 4(a)–(c)) and the summer sea ice melting in KR (green lines in figures 4(a)–(c)). Around the middle of the 21st century, with the vanish, slowdown, or continuous intensification of sea ice melting variations, AASV also disappears under SSP1-2.6, decreases under SSP2-4.5 and maintains under SSP5-8.5 accordingly. This suggests that the intensity of AASV is closely related to the summer SIE variations. Under SSP1-2.6 scenario (figure 4(d)), in the first half of the 21st century, AASV and SIE variations show a significant positive correlation, while in the second half of the 21st century, when AASV and SIE change close to zero, the correlation between them almost disappeared. A similar phenomenon can be observed under SSP2-4.5 scenario (figure 4(e)). When global warming tends

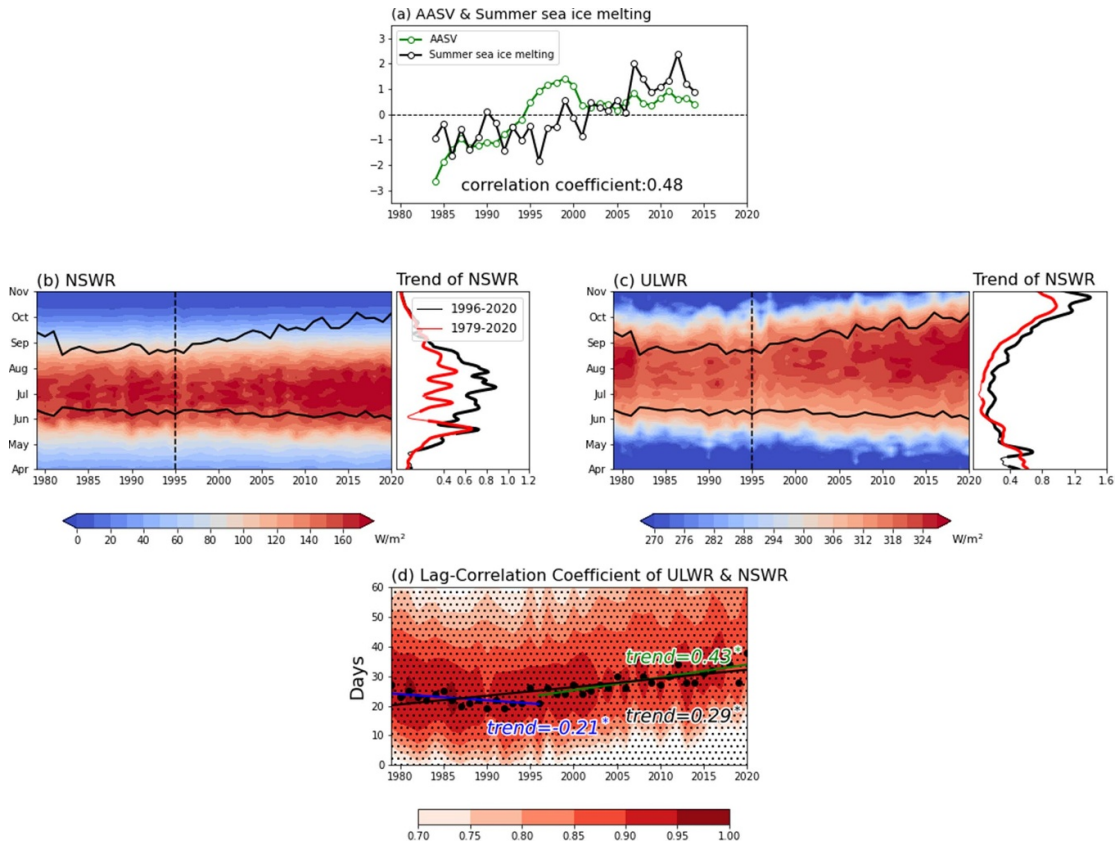

Figure 2. (a) The standardized AASV and summer Sea ice melting. (b) The daily NSWR (negative upward) and its trend (black for 1996–2020, red for 1979–2020). Bold parts show significant values at the 99% confidence level. (c) is the same as (b) but for daily ULWR (positive upward). (d) Distribution of lag-correlation coefficient between ULWR and NSWR. The black dots are the lag days corresponding to the maximum lag-correlation coefficient of a year. Dotted areas and the trend value with asterisk show significant values at the 99% confidence level.

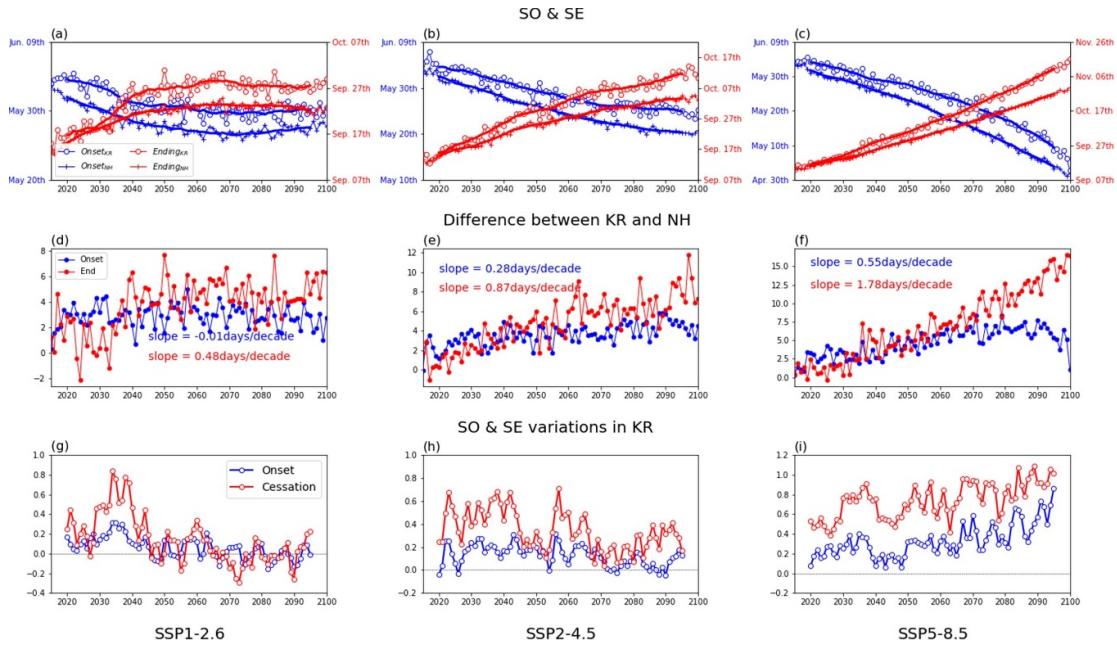

Figure 3. (a) The SO (blue lines) and SE (red lines) in KR (line with circles) and NH (line with plus signs). (d) Difference of the SO (blue lines) and SE (red lines) between KR and NH (in unit of days). (g) SO and SE variations in KR (in unit of 10^6 km^2). (a), (d), (g) are results under SSP1-2.6. (b), (e), (h) and (c), (f), (i), are same as (a), (d), (g), but for SSP2-4.5 and SSP5-8.5.

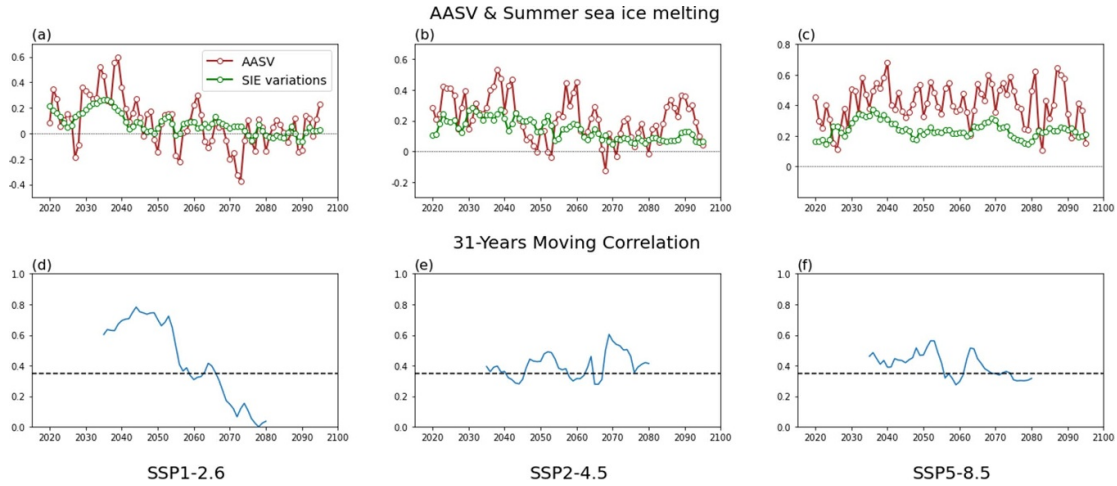

Figure 4. (a) The standardized AASV (brown line) and summer sea ice melting in KR (green line). (d) 31 year moving correlation between AASV and summer SIE variations in KR. Dash lines in (d) denote the significant values at the 95% confidence level. (a), (d) are results under SSP1-2.6. (b), (e) and (c), (f) are same as (a), (d) but for SSP2-4.5 and SSP5-8.5.

to stabilize, the sea ice melted in summer will no longer increase (the SIE variations tend to zero), and the correlation between AASV and summer sea ice melting begins to decline significantly. Under the SSP5-8.5 scenario (figure 4(f)), due to the continuous intensification of global warming, the summer sea ice melting is maintained at a high level, and the sliding correlation between AASV and SIE changes is also maintained around 0.37. The sliding correlation coefficients between AASV and SIE show different changes under the three scenarios. This does not mean that their relationship is sensitive to future radiative forcing, but it indicates the coexistence relationship between the two. In other words, AASV occurs in the area where sea ice melts violently in summer. When the melting is no longer intensified, AASV disappears. Based on this relationship, especially under the SSP5-8.5 scenario, when the region with severe sea ice melting moves from the edge of the Arctic to the center, the region with the most significant occurrence of AASV also moves to the center of the Arctic (figure S4). It is suggested that future work should consider capturing AASV dynamically rather than exploring AASV variations in fixed areas. In general, the shortening of the previous sea ice recovery period (delayed SE of the previous year and the advanced SO of the current year) exacerbates the summer sea ice melting, which may further strengthens the AASV.

In terms of the sliding correlation coefficient between AASV and summer sea ice melting, they influence each other. It is clear that the longer summers lead to an increase in the summer sea ice melting, while it is worth noting that the increased sea ice melting also further lengthens the summer, particularly delaying the SE rather than causing the SO to start earlier. Although it is difficult to capture the effects of AASV in short-term observations, it can be found that AASV is likely to have severe impacts on the arctic climate and ecology based on future simulations. The continuous strengthening of AASV will significantly reduce the length of the SIE recovery period, especially under the SSP2-4.5 and SSP5-8.5. Figures 5(a)–(c) show the daily SIE variations in KR (the value of each grid is the difference between the SIE on that day and the SIE of the previous day in KR). It can be found that the most intense melting will almost occur in July-August, with no significant advance. However, the time of maximum sea ice recovery will significantly delay, especially under SSP5-8.5. It is projected to delay from November to February of the next year. On the one hand, AASV makes the timing of SIE entering a rapid recovery period be delayed (delay about 1 month under SSP2-4.5 (figure 5(b)), and about 2–3 months under SSP5-8.5 (figure 5(c)). On the other hand, AASV also results in a shorter time for SIE to remain at a higher level, leaving less time for the sea ice to grow thick and making it more likely to disappear in the coming year. Furthermore, the relationship between AASV and summer melting could greatly affect the Arctic amplification effect (figures 5(d)–(f)). Regardless of the intensity variations, the appearance and peak time of Arctic amplification will be significantly delayed by almost the same time with the delay of sea ice recovery. While the weakest Arctic amplification still occurs in June-August, hardly in advance. Although only the temperature gradient in the lower troposphere between the Arctic and mid-high latitudes of the NH during the occurrence of the Arctic amplification effect is reduced (Screen and Simmonds 2013, Dai *et al* 2019), it is worth further investigating whether its effect on the weather in the middle latitudes has a seasonal change.

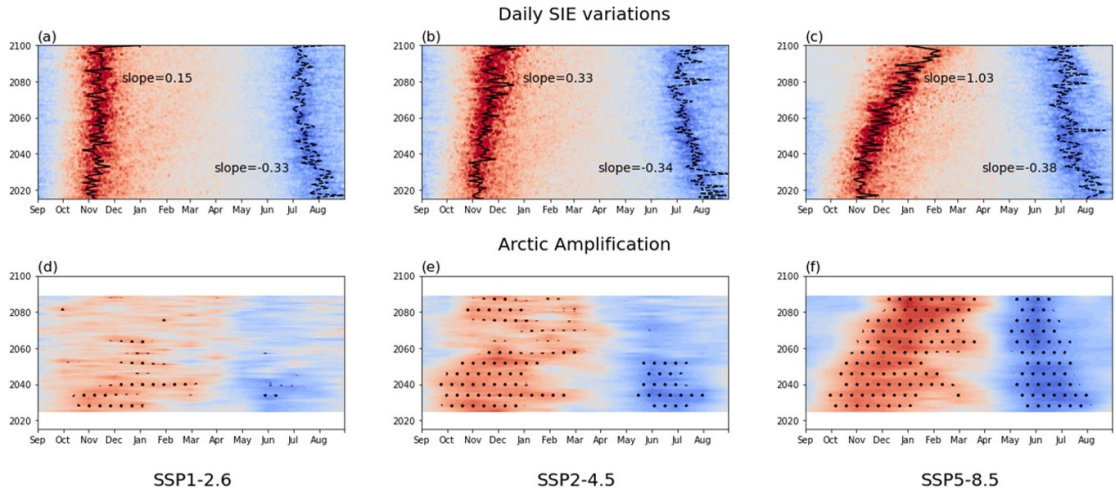

Figure 5. (a) Daily SIE variations (in unit of 10^6 km^2) (a) and Arctic Amplification (in unit of K/year) (d) under SSP1-2.6. (b), (e) and (c), (f) are same as (a), (d) but for SSP2-4.5 and SSP5-8.5. The solid and dotted black lines represent the maximum and minimum values, respectively. Dotted areas in (d), (e) and (f) show significant values at the 95% confidence level.

4. Conclusion and discussion

This paper investigates the feedback between AASV and summer sea ice melting based on reanalysis, observations and CMIP6 simulations. Unlike previous studies using daily melting, here we take the 75th percentile of the daily SAT as the threshold to determine the SO and SE. It could be found that the rate of delayed SE is significantly higher than earlier SO in areas with significant sea ice melting. Enhanced sea ice melting, the main contributor to AASV, increases the ability of the oceans to absorb more shortwave radiation in summer and then release more energy to heat the lower atmosphere later. To overcome the temporal limitations of observations, we used 21st century simulations of CMIP6 to capture AASV variability and investigate the role of sea ice melting in it. In CMIP6 simulations, AASV gets stronger (weaker) as sea ice melt increases (decreases) and disappears when the sea ice melting trend stalls. Especially under the scenario of SSP5-8.5 with the aggravation of global warming, the enhanced AASV contributes to the shortening of the sea ice recovery period and further promotes the acceleration of sea ice melting, which reflects the positive feedback between AASV and sea ice melting.

AASV significantly contributes to the Arctic summer extension and determines its direction, providing a reference for the schedule of the Arctic route (Wei *et al* 2020) as well as causing more damage to the Arctic ecology. The positive feedback between AASV and sea ice melting not only affects local summer variations in the Arctic but also may affect the weather and climate on a larger scale (Overland *et al* 2011, Screen and Simmonds 2013, Cohen *et al* 2014, Luo *et al* 2018). For example, AASV is likely to delay the onset and peak time of the Arctic amplification effect by 1–2 months in the late 21st century. Therefore, further research is needed to determine how such changes might affect the winter-spring climate in mid-high latitudes. In addition, key issue for future studies is to design more sensitivity experiments and use the sea ice data with a higher temporal resolution to quantify the relationship between AASV and sea ice melting.

Data availability statement

The data that support the findings of this study are openly available at the following URL/DOI: https://psl.noaa.gov/data/gridded/data.ncep.reanalysis.html, https://esgf-node.llnl.gov/projects/cmip6/, http://climexp.knmi.nl/showmap.cgi, https://ceres.larc.nasa.gov/ and https://nsidc.org/.

Acknowledgments

This research is supported by the National Key Research and Development Program of China (2022YFF0801704) and the National Natural Science Foundations of China (42175035; 41831174). The data analysis in this paper were conducted on the supercomputing system in the Supercomputing Center of Nanjing University of Information Science and Technology.

Conflict of interest

Xiaoye Yang, Gang Zeng, Wei-Chyung Wang, Vedaste Iyakaremye, Shiyue Zhang declare that they have no conflict of interest.

ORCID iD

Vedaste Iyakaremye https://orcid.org/0000-0001-6791-1464

References

Biss A and Anderson M 2014 Snowmelt onset over Arctic sea ice from passive microwave satellite data: 1979–2012 *Cryosphere* **8** 2089–100

Cohen J *et al* 2014 Recent Arctic amplification and extreme mid-latitude weather *Nat. Geosci.* **7** 627–37

Dai A, Luo D, Song M and Liu J 2019 Arctic amplification is caused by sea-ice loss under increasing CO_2 *Nat. Commun.* **10** 121

Davy R, Chen L and Hanna E 2018 Arctic amplification metrics *Int. J. Climatol.* **38** 4384–94

Ding Q *et al* 2017 Influence of high-latitude atmospheric circulation changes on summertime Arctic sea ice *Nat. Clim. Change* **7** 289–95

Francis J and Wu B 2020 Why has no new record-minimum Arctic sea-ice extent occurred since September 2012? *Environ. Res. Lett.* **15** 114034

Huang F, Zhou X and Wang H 2017 Arctic sea ice in CMIP5 climate model projections and their seasonal variability *Acta Oceanol. Sin.* **36** 1–8

Johannessen O, Kuzmina S, Bobylev L and Miles M 2016 Surface air temperature variability and trends in the Arctic: new amplification assessment and regionalization *Tellus* **68** 28234

Kalnay E *et al* 1996 The NCEP/NCAR 40-year reanalysis project *Bull. Am. Meteor. Soc.* **77** 437–71

Kwok R, Cunningham G, Wensnahan M, Rigor I, Zwally H and Yi D 2009 Thinning and volume loss of Arctic sea ice: 2003–2008 *J. Geophys. Res.* **114** C12024

Luo D, Chen X, Dai A and Simmonds I 2018 Changes in atmospheric blocking circulations linked with winter Arctic sea-ice loss: a new perspective *J. Clim.* **31** 7661–78

Markus T, Stroeve J and Miller J 2009 Recent changes in Arctic sea ice melt onset, freeze-up, and melt season length *J. Geophys. Res.* **114** C12024

Miles M, Divine D, Furevik T, Jansen E, Moros M and Ogilvie A 2014 A signal of persistent Atlantic multidecadal variability in Arctic sea ice *Geophys. Res. Lett.* **41** 463–9

Notz D and Stroeve J 2016 Arctic sea ice loss directly follows cumulative anthropogenic CO_2 emissions *Science* **354** 6313

Omrani N, Bader J, Keenlyside N and Manzini E 2016 Troposphere–stratosphere response to large-scale North Atlantic Ocean variability in an atmosphere/ocean coupled model *Clim. Dyn.* **46** 1397–415

Overland J, Wood K R and Wang M 2011 Warm Arctic—cold continents: climate impacts of the newly open Arctic Sea *Polar. Res.* **30** 15787

Peings Y and Magnusdottir G 2014 Response of the wintertime Northern Hemisphere atmospheric circulation to current and projected Arctic sea ice decline: a numerical study with CAM5 *J. Clim.* **27** 244–64

Perovich D K, Jones K F, Light B, Eicken H, Markus T, Stroeve J and Lindsay R 2011 Solar partitioning in a changing Arctic sea-ice cover *Ann. Glaciol.* **52** 192–6

Perovich D K, Richter-Menge J A, Jones K F and Light B 2008 Sunlight, water, and ice: extreme Arctic sea ice melt during the summer of 2007 *Geophys. Res. Lett.* **35** L11501

Perovich D and Polashenski C 2012 Albedo evolution of seasonal Arctic sea ice *Geophys. Res. Lett.* **39** L08501

Screen J A and Simmonds I 2010 The central role of diminishing sea ice in recent Arctic temperature amplification *Nature* **464** 1334–7

Screen J and Simmonds I 2013 Exploring links between Arctic amplification and mid-latitude weather *Geophys. Res. Lett.* **40** 959–64

Serreze M, Crawford A, Stroeve J, Barrett A and Woodgate R 2016 Variability, trends and predictability of seasonal sea ice retreat and advance in the Chukchi Sea *J. Geophys. Res.* **121** 7308–25

Serreze M and Stroeve J 2015 Arctic Sea Ice Trends, variability and implications for seasonal ice forecasting *Phil. Trans. R. Soc. A* **373** 20140159

Stroeve J, Markus T, Boisvert L, Miller J and Barrett A 2014 Changes in Arctic melt season and implications for sea ice loss *Geophys. Res. Lett.* **41** 1216–25

Stroeve J and Notz D 2018 Changing state of Arctic sea ice across all seasons *Environ Res. Lett.* **13** 103001

Sun C, Li J and Zhao S 2015 Remote influence of Atlantic multidecadal variability on Siberian warm season precipitation *Sci. Rep.* **5** 16853

Taylor P, Cai M, Hu A, Meehl J, Washington W and Zhang G 2013 A decomposition of feedback contributions to polar warming amplification *J. Clim.* **26** 7023–43

Wang J, Guan Y, Wu L, Guan X, Cai W, Huang J Dong W and Zhang B.2021 Changing lengths of the four seasons by global warming *Geophys. Res. Lett.* **48** e2020GL091753

Wei T, Yan Q, Qi W, Ding M and Wang C 2020 Projections of Arctic sea ice conditions and shipping routes in the twenty-first century using CMIP6 forcing scenarios *Environ. Res. Lett.* **15** 104079

Zhang R 2015 Mechanisms for low-frequency variability of summer Arctic sea ice extent *Proc. Natl Acad. Sci. USA* **112** 4570–5